Eidgenössische Technische Hochschule Zürich

Institut für Geodäsie
und Photogrammetrie

Bericht

252

Digital Line Photogrammetry

Concepts, Formulation, Degeneracies, Simulations, Algorithms, Practical examples

P. Patias

E. Petsa

A. Streilein

Dezember1995

DIGITAL LINE PHOTOGRAMMETRY

Concepts, Formulation, Degeneracies, Simulations, Algorithms, Practical examples

P. PATIAS
Department of Cadastre, Photogrammetry and Cartography
The Aristotle University of Thessaloniki, Greece

E. PETSA
Department of Surveying
National Technical University of Athens, Greece

A. STREILEIN
Institute of Geodesy and Photogrammetry
Swiss Federal Institute of Technology
ETH-Hoenggerberg, Zurich, Switzerland

IGP Bericht Nr. 252

Digital Line Photogrammetry
Concepts, Formulation, Degeneracies, Simulations,
Algorithms, Practical examples

Petros Patias,
Elli Petsa,
André Streilein

ISBN 3-906513-73-4

FOREWORD

Some of the study and research work as well as part of the processing of the practical example contained in this report was performed while Prof. Dr. P. Patias spent four months of his sabbatical leave at our Institute as a guest professor in 1994.

The subject of line photogrammetry (especially straight line photogrammetry), although not a new item as such, has found increased attention during the past decade. This interest, partly triggered by the desire for refinement and completion of the geometrical aspects of sensor orientation, was generated even more than that by the specific conditions of digital photogrammetry, where, prior to the completed orientation of images, point correspondences are sometimes hard to establish automatically. In addition, certain applications, e.g. indoor robotics or architectural photogrammetry, provide usually for a wealth of well detectable line features, which should be used to at least stabilize, if not enable orientation, navigation and so forth.

This report encompasses key aspects related to the mathematical formulation of straight line photogrammetry, space resection and relative orientation. Results from a practical example (CIPA project „Otto Wagner Pavillon" in Vienna) complete the essay.

It is planned to include the procedure of straight line processing, as outlined in this report, in our software package DIPAD (**Di**gital **P**hotogrammetry and **A**rchitectural **D**esign) in order to enhance its functionality.

I am very pleased about this excellent piece of work, which is both innovative and of practical relevance. This is to express my sincerest thanks to the authors for their very interesting contributions.

Zürich, December 1995 A. Gruen

Acknowledgements

This report has been produced during the stay of the first author as a guest professor at the Institute of Geodesy and Photogrammetry, ETH Zürich, June 1994 through September 1994. The first author would like to express his thanks to the Institute and his colleagues there for their hospitality and help. The availability of computer, data and other resources to our disposal, during this study is also gratefully acknowledged.

CONTENTS

	page
FOREWORD	1
Acknowledgements	2
1. INTRODUCTORY CONCEPTS OF LINE PHOTOGRAMMETRY	5
2. MATHEMATICAL FORMULATION OF LINE PHOTOGRAMMETRY	8
2.1. Image Line definition	10
2.1.1. Line definition by two points	10
2.1.2. Line definition by slope and intercept	10
2.1.3. Line definition by two intercepts	11
2.2. Choice of mathematical model	12
3. SPACE RESECTION USING STRAIGHT LINE FEATURES	14
3.1. Determination of sensor attitude	15
3.1.1. Critical configurations - Degeneracies	15
3.1.2. Minimum control requirements	17
3.1.3. Accuracy assessment	18
3.1.3.1. Convergence rate	18
3.1.3.2. The role of geometry	19
3.1.3.3. The role of number of lines	21
3.1.3.4. Accuracy of rotational elements	24
3.2. Determination of sensor location	25
3.2.1. Critical configurations - Degeneracies	25
3.2.2. Minimum control requirements	27
4. RELATIVE ORIENTATION USING STRAIGHT LINE FEATURES	28
4.1. The case of the stereopair	28
4.2. The case of image triples	29
4.3. Determination of relative orientation parameters	30
4.3.1. Rotational parameters	30
4.3.2. Translational parameters	32
4.4. Critical configurations - Degeneracies	33
4.5. Simulated example	37

5. A PRACTICAL EXAMPLE 39
5.1. The Object 39
5.2. Image acquisition 40
5.3. Extraction and correspondance of straight lines 41
5.4. Determination of exterior orientation 45

6. CONCLUDING REMARKS 49

REFERENCES 51

1

INTRODUCTORY CONCEPTS OF LINE PHOTOGRAMMETRY

For good reasons, the discrete point is the entity around which Photogrammetry has basically constructed its mathematical models and algorithms (in other fields dedicated to the study of shape, limitations of being "bound to points" were clearly recognized; eg. *Bookstein, 1978*).

Although images contain a wealth of feature information, photogrammetrists attempt to locate points on these images, which are mainly intersections of features. *Masry (1981)* in an early work recognized the kind of problems that may be encountered in such situations, which worth quoting here:

" • A number of features exist but the number of intersection points is not sufficient for the application.
- The features do not intersect within the bounds of the image dealt with.
- The intersections are not well defined.
- The intersection points are poorly distributed, which may result in an ill-conditioned solution for the transformation parameters. "

and concludes that "A poor solution may consequently be the result, despite the availability of the features themselves and the user's ability to relate the image to the map visually using those same features".

These problems motivated a number of researchers over the last years to use other types of object descriptors than points (e.g. *Mulawa and Mikhail, 1988; Mulawa, 1989*). These descriptors/features will act as agents of 2D-3D and 2D-2D correspondences

and attract growing interest. Among these, linear features, and straight lines in particular, are an obvious choice.

In conventional Photogrammetry, the use of straight line for image orientation may reduce fieldwork or provide solutions in the absence of control points. The application reported by *Doehler (1975)* is an early example for this use. The well established plumb-line method for partial camera calibration, now also adapted for aerial photogrammetry (*Fryer and Goodin, 1989*), is another. The authors have successfully employed vanishing points of straight lines for the digital rectification of old amateur photographs of building facades demolished long ago (*Karras et. al., 1993*). Finally, close-range photogrammetric packages optionally requiring straight lines, rather than points, as object control could seem friendlier to non-expert users (eg. architects).

But it is chiefly the advent of Digital Photogrammetry and the prospect of replacing human operators by automated image analysis which pushes today towards linear rather than point features. Notwithstanding the fact that effective linear feature extraction and correspondence still remains a thorny problem, (unsignalized) lines are generally easier to detect and extract robustly in automated processes, simplifying thus questions of correspondences, reducing computational cost and limiting matching ambiguities in 3-D reconstruction. Line fitting along redundant points of (preferably long) edges may allow recovery of location and orientation of linear features with subpixel accuracies (*Liu and Huang, 1988; Mitichie and Habelrih, 1989; Huang, 1990; Liu et al., 1990; Hekkila, 1991; Tommaselli and Tozzi, 1992; Weng et al., 1992*).

One could regard lines, after *Hekkila (1991)*, as natural descriptors for Digital Photogrammetry. Hence, they can be or are being employed as basic entities in tasks involving monoscopic or polyscopic imagery and as varying as rectification, camera calibration, relative orientation, space resection and object reconstruction, estimation of motion or mobile robot navigation in the fields of terrestrial, aerial and satellite photogrammetry, computer vision and robot vision (*Masry, 1981; Liu and Huang, 1988; Finsterwalder, 1991; Heikkinen and Laiho, 1992; Tommaselli and Tozzi, 1992; Weng et al., 1992; Strunz, 1992(a); 1992(b), 1993, Zielinski, 1992: Petsa and Patias, 1994(b)*).

Of course this type of approach offers a lot of advantages, like improved measurement accuracy in the context of full automation, as pointed out by many researchers: "Generally, line features are easier to extract in a noisy image than point features.

Furthermore, it is easier to determine the position and orientation of a line to sub-pixel accuracy than the coordinates of a point" (*Liu and Huang, 1988*).

On the other hand, it also involves a number of newly set issues to be answered, like the development of proper mathematical formulations, the study of the minimum requirements, the study of degeneracy cases and the study of special space configurations (like parallelity, perpendicularity, angularity, collinearity, coplanarity, combinations of these, and the like) involving lines.

Our starting point is the assumption that straight lines have already been recognized and extracted from the digital images. Furthermore, we assume that homologous lines in overlapping images have been matched. Although, we do not underestimate the problems involved in the above procedures, we realize that these issues attract the research interest of many researchers, from many disciplines and for many years ("Research on edge detection including straight line extraction can be traced back to at least 20 years. ..... In many computer vision systems, line extraction is followed by finding matches or correspondences of lines over several images. Once correspondences are obtained, more higher level processes, such as object recognition and motion analysis can be performed." (*Liu and Huang, 1990)*). Some of these algorithms seem to be particularly suitabie for Line Photogrammetry(e.g. *Canny, 1986; Burns, et. al., 1986; Nalwa and Binford, 1986*), since they can extract lines of particular orientation, or filter out orientations, which as we will see later on, lead to critical situations. Additionally, many algorithms for straight line matching have been presented over the last years (e.g. *Medioni and Nevadia, 1984; Price, 1984; McIntosh and Mutch, 1988; Liu and Huang, 1990*). Therefore, it is our opinion that Photogrammetry has a lot to benefit from all this effort in the near future.

2

MATHEMATICAL FORMULATION OF LINE PHOTOGRAMMETRY

Straight lines ***L*** in object space XYZ and lines ***l*** in the image plane xy define with the perspective center O(X_O, Y_O, Z_O) the two projection planes ε and ***E*** respectively (Figure 1). The condition for ***l*** to be the perspective image of line ***L*** is the coincidence of ε and ***E***.

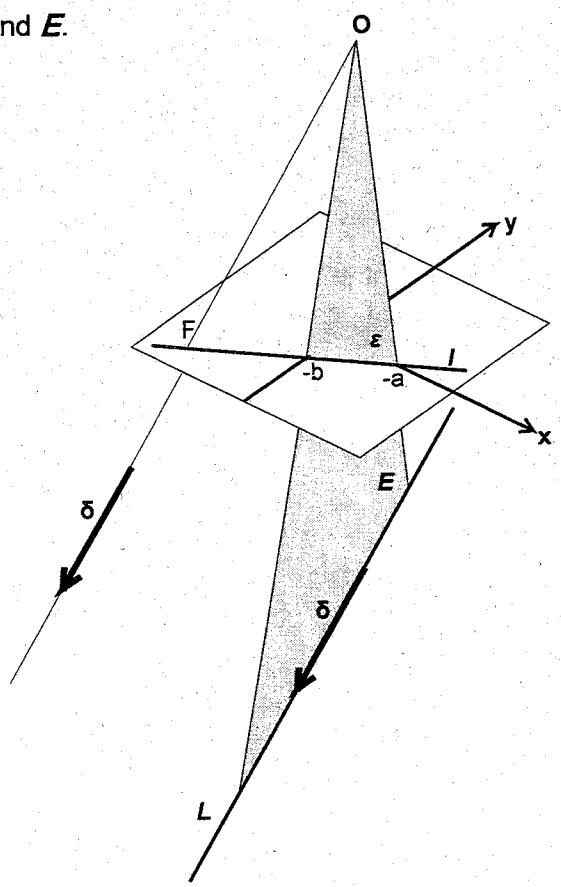

Figure 1: Projective geometry in Line-based Photogrammetry.

Let object line $\boldsymbol{L}$ be described by the parametric equation (1)

$$\mathbf{q} = \mathbf{p} + s\boldsymbol{\delta} \qquad (1)$$

with

$\mathbf{q}^T = [\ X-X_o,\ Y-Y_o,\ Z-Z_o\ ]$ for any point (X,Y,Z) of line $\boldsymbol{L}$
$\mathbf{p}^T = [\ X-X_p,\ Y-Y_p,\ Z-Z_p\ ]$ for a reference point P on line $\boldsymbol{L}$
$\boldsymbol{\delta}^T = [\ L,\ M,\ N\ ]$ the direction vector of line $\boldsymbol{L}$
s = a scalar length parameter

It should be noted here that the description of the line through the above six parameters is not unique, since it depends both on the selection of the "initial" point P and the length of the vector $\boldsymbol{\delta}$. Thus we need to impose two conditions, one involving the parameters (x_p y_p z_p) and another one involving the parameters (L M N). Then the line will be correctly described by 4 parameters.

Such conditions are of the form:

$$\begin{aligned} G_1(x_p\ ,\ y_p\ ,\ z_p) &= 0 \\ G_2(L\ ,\ M\ ,\ N) &= 0 \end{aligned} \qquad (1a)$$

and different such conditions can be imposed, eg.

G_1: $x_p = 0$; or $y_p = 0$; or $z_p = 0$; or $Lx_p + My_p + Nz_p = 0$

and (1b)

G_2: $L = 1$; or $M = 1$; or $N = 1$; or $L^2 + M^2 + N^2 = 1$

The equation of plane $\boldsymbol{E}$ is

$$\mathbf{q} \cdot (\mathbf{p} \times \boldsymbol{\delta}) = \mathbf{q}^T \mathbf{J} = 0 \qquad (2)$$

with $\mathbf{J}$ being the normal vector to plane $\boldsymbol{E}$. Denoting by $\mathbf{j}$ the normal vector of plane $\boldsymbol{\varepsilon}$, the condition for planes $\boldsymbol{\varepsilon}$ and $\boldsymbol{E}$ to be coincident is the collinearity condition between $\mathbf{J}$ and $\mathbf{j}$:

$$\mathbf{j} = \lambda \mathbf{R}\,\mathbf{J} = \lambda\,\mathbf{G} \qquad (3)$$

whereby

R denotes the image rotation matrix
λ is a scale factor, and
$\mathbf{G}^T = (\mathbf{R}\,\mathbf{J})^T = [\,U, V, W\,]$

Depending on the description of the image line ***l*** (i.e. through two distinct points, through slope and intercept, or through two intercepts), different expressions for the normal vector **j** of $\boldsymbol{\varepsilon}$, resulting in three alternative forms of eq. (3) are finally obtained as follows.

2.1. Image Line definition

2.1.1. Line definition by two points

Assuming that the line ***l*** in the image plane is defined by two points (x_i, y_i) and (x_j, y_j) then :

$$\mathbf{j}^T = [\; c\Delta y_{ij} \quad , \quad -c\Delta x_{ij} \quad , \quad y_i x_j - y_j x_i - \Delta y_{ij} x_o + \Delta x_{ij} y_o \;]$$

The camera constant c and the principal point coordinates (x_o, y_o) are the three inner orientation parameters. Elimination of scale factor λ in eq. (3) finally yields for each point an equation of the form :

$$(x - x_o)\,U + (y - y_o)\,V - c\,W = 0 \qquad (4)$$

2.1.2. Line definition by slope and intercept

Expressions of line **l** in parametric form as

$y = x\,t - b$

or

$x = y/t - a$

result in

$j^T = [\, c\,t \quad , \quad -c \quad , \quad b - x_o t + y_o \,]$

or

$j^T = [\, -c \quad , \quad c / t \quad , \quad a - x_o + y_o/t \,]$

respectively. The respective forms of eq. (3) now become :

$$-t = \frac{U}{V} \qquad b = -c\frac{W}{V} - x_o\frac{U}{V} - y_o$$

$$-\frac{1}{t} = \frac{U}{V} \qquad a = -c\frac{W}{V} - x_o - y_o\frac{U}{V} \tag{5}$$

2.1.3. Line definition by two intercepts

Representing, finally the image line *l* by the parametric form

$$\frac{x}{a} + \frac{y}{b} + 1 = 0$$

then (see also Fig. 1) the following holds :

$j^T = [\, -c\,b \quad , \quad -c\,a \quad , \quad a\,b + b\,x_o + a\,y_o \,]$

In this case the elimination of λ in eq. (3) results in the form :

$$a = -c\frac{W}{U} - x_o - y_o\frac{V}{U} \qquad b = -c\frac{W}{V} - x_o\frac{U}{V} - y_o \tag{6}$$

Equations (4) - (6) are derived from the basic collinearity equation (3) of Line Photogrammetry. In fact, eq. (4) is basically equivalent to the formulation of *Mulawa (1989)* and eq. (6) to that of *Tommaselli and Tozzi (1992)*. In the forms presented here, however, they have been extended to incorporate the three inner orientation elements c, x_o, y_o. Thus in the above general forms they are suitable for the employment of

straight line features in all three fundamental tasks of photogrammetry, namely camera calibration, space resection, and space intersection.

The difference between eq. (4) and eq. (6) is that the first one assumes that **observations are performed on points** of the linear features. The second one assumes that the **observables are the parameters of the image lines**. But most importantly both assume correspondence of linear features within different images and **not correspondences of individual points** as in conventional Photogrammetry. This is quite important, as pointed out in (*Mulawa and Mikhail, 1988*) "It is critical to point out that in dealing with features, for example line segments, we must be so general as to assume no point correspondences. Thus, a line feature on the ground may be represented by two different line segments, one on each of two images, where one represents an object segment totally different from that represented by the other".

2.2. Choice of mathematical model

In applications of computer vision, extraction of straight lines mostly results in a parametric expression after line fitting to redundant edge points; the image space line parameters are subsequently related to those of the object space line. Contrary to this, in the model of eq. (4) it is not the derived quantities but the originally observed image point coordinates x, y themselves which are used for a direct form fitting of the lines in object space, bypassing the stage of image feature reconstruction. Advantages of such an approach, particularly for space intersection, have been outlined by *Mulawa (1989)* and *Heikkila (1991)*.

However, at least in the case of straight lines, a preceding image line reconstruction and the subsequent use of the derived image line parameters as observations, may have their own merits. In space resection and camera calibration, for instance, but also in multiple space intersection it may be more meaningful to detect (and exclude) "outlying" lines rather than noisy observations of isolated points.

Straight line features can be outliers in the adjustment basically for three reasons: *First*, unstable extraction of image lines. This can be detected in the course of line fitting; each line can then be assessed separately regarding its stability and precision. *Second*, image linearity is disturbed not only by the "random" errors of extraction, but also by possible systematic errors of the imaging and recording systems. Line fitting in

the image space has been proven useful for estimating lens and image distortions. *Third*, particular lines may well appear as outliers also because of the "object control lines" themselves, e.g. due to inaccuracies in their parameters, due to their deviations of assumed verticality, horizontality, etc., or even linearity itself. Interpretation of such phenomena is easier when having adopted "compact" models involving only few derived observations rather than the numerous original ones.

Obviously, this question is open to different answers. The above, however, represent aspects of the merits the image line-to-object line correspondence might have compared to image point-to-object line relationship. In the light of the above discussion in the following chapters only eq. (6) is used. Regarding eq. (6) the following should be observed:

- If the initial values of the rotational elements of the exterior orientation are all zero ($\omega = \varphi = \kappa = 0$) and the object space line is horizontal ($L = 1, M = N = 0$) whence *U becomes zero*

or

- if the image line runs parallel to the image axis x whence *a becomes infinite*,

then

the first equation of (6) is written in the form $-t = 0$ or $U = 0$ respectively, and accordingly for the second equation.

To tackle such cases, provision should taken by *artificially rotating the image coordinates about the lens axis* (swing κ in standard photogrammetric notation).

3

SPACE RESECTION USING STRAIGHT LINE FEATURES

In the computer vision literature the space resection problem is usually split, for linearization purposes, into two distinct phases; recovery of rotational parameters and translational parameters (eg. *Huang, 1990; Strunz, 1993*). But recovery of the attitude information only, i.e. "Partial Space Resection" is crucial for photogrammetry for further reason too. The equations for space resection given above require object lines of known orientation as well as location, which obviously demands a certain amount of field work. It is much easier and practical, on the contrary, to know or assume only their orientation in object space. This knowledge suffices not merely for the recovery of rotations but also for camera calibration purposes.

On the other hand, recovered image rotations, particularly when combined with known scaling distances, represent information sufficient for many photogrammetric tasks (e.g. rectification, object reconstruction in an arbitrary system) or providing providing approximate values for others (e.g. space resection, relative orientation, initial orientation of convergent images for image matching). An interesting application is also the combination of the recovered attitude information with GPS positional measurements in aerial photogrammetry (*Petsa and Patias, 1994b*).

3.1. Determination of sensor attitude

Assume only the direction vector $\boldsymbol{\delta}^T = [\ L, M, N\ ]$ of object line L to be known. The intersection of the corresponding image line l with a line parallel to L through the projection center O is the vanishing point $F(x_F, y_F)$ (Fig. 1).

The vectors $\mathbf{f}^T = [\ x_F - x_o \quad , \quad y_F - y_o \quad , \quad -c\ ]$ and $\boldsymbol{\delta}$ satisfy the collinearity condition:

$$\mathbf{f} = \lambda \mathbf{R}\, \boldsymbol{\delta}$$

thus resulting in

$$x_F = x_o - c\frac{U}{W} \qquad y_F = y_o - c\frac{V}{W}$$

Introduction in the intercept equation (6) of image line l yields :

$$c\,b\,U + c\,a\,V - (a\,b + b\,x_o + a\,y_o)\,W = 0 \qquad (7)$$

or equivalently

$$\mathbf{j}^T \mathbf{R}\ \boldsymbol{\delta} = 0 \qquad (7a)$$

which directly expresses the orthogonality of the vectors $\mathbf{j}$ and $\boldsymbol{\delta}$ (*Huang, 1990*).

Equation (7) connects the image space line l parameters (a, b) with the object space line L parameters (L, M, N) through the rotational parameters (ω, φ, κ). Every observed image line l contributes with one condition equation of the form (7). **Therefore 3 known object space lines L seems to be the minimum requirement for the determination of the three rotations ω, φ, and κ.**

3.1.1. Critical configurations - Degeneracies

Regarding the possible number of solutions for the angles ω, φ and κ, earlier studies have indicated that the maximum number n of solutions, using the minimum number of

lines $N_{min} = 3$ is $n(N_{min})_{max} \leq 8$. It is not known under which conditions this n_{max} multiplicity of solutions occur; neither are known the conditions for the non-uniqueness degeneracy or the exact number n of solutions for N = 4 lines; "some parallelism conditions" are responsible for that (*Huang, 1990*; see also *Strunz, 1993*). *Dhome et al. (1989)* have used cube junctions and found up to n = 8 solutions. Our investigation on the existence of multiple solutions for the matrix $\mathbf{R}$ showed (*Petsa and Patias, 1994(a)*) that actually holds $\mathbf{n(N_{min})_{max} = 8}$.

The general case of 3 lines of random angular configuration is difficult to investigate geometrically or algebraically. Until now, the question has been investigated with extensive tests based on simulated, highly divergent object line configurations (*Petsa and Patias, 1994(a)*). However, with geometric reasoning we have investigated non-uniqueness of solution in cases of special configurations where parallelism and perpendicularity of lines exist.

Based on simulation results, the following conclusions have been drawn:

- *3 random lines yield a total of 4 solutions, each one of which provides different triples of vanishing points F_i of object lines L_i on the corresponding image lines l_i; whether object lines intersect or not is irrelevant.*

- *When the 3 lines are all orthogonal to each other then, and only then, the solutions are 8; to these correspond 2 sets of vanishing points, one to every four of them.*

- *When the 3 object lines are parallel to each other then, and only then, the image rotations remain indefinite.*

- *3 lines, of which 2 are parallel, provide 4 solutions to which correspond two vanishing points of the third line.*

- *2 parallel lines perpendicular to a third provide 4 solutions to which corresponds a unique vanishing point of the third line.*

- *2 perpendicular lines and a third of random direction provide 4 solutions to which correspond 4 triples of vanishing points.*

A selection of these simulation, referring to 4 lines, basically considering varying geometries involving parallelism and perpendicularity, are given in Table 1 by way of illustration.

Table 1: Number of solutions for rotation matrix **R** when N=4 lines used

Number of solutions for the Rotation matrix (**rnd**: random **prl**: parallel **prp**: perpendicular)	
Straight line configuration	*Solutions*
4 rnd	1
3 prp + 1 rnd	1
2 prp + 2 rnd	1
2 prl + 2 rnd	1
2 prl + 1 prp to it + 1 rnd	1
2 prl + 2 non prl, prp to these	4
2 prl + 2 prl, prp to these	4
2 prl + 2 prl, non prp to these	4

3.1.2. Minimum control requirements

Generally, as shown above, 3 object lines of any angular configuration lead to either an infinite number of solution (parallelism) or non-uniqueness of 8 solutions (orthogonality) or 4 solutions (all remaining cases).

The minimum requirements for uniquely recovering the image rotations is a configuration of 4 straight object lines defining at least 3 different directions in object space. If the direction defined by the 4 lines are only 3 (parallelism of 2 lines), these 3 directions must not be orthogonal to each other. Any other directional relationship of 4 object straight linear features in object space provide a unique solution for the angles ω,φ and κ.

Investigations regarding critical configurations, degeneracy and minimal requirements are absolutely necessary for fully grasping geometry in configurations likely, but also unlikely, to emerge and avoiding possible ambiguities or errors. Inevitably based on algebra and geometry, however, they refer to "abstractions" of reality.

In the investigations referred to, for instance, lines may in fact have been imaged from any viewpoint, i.e. objects are considered transparent and consisting of endless lines. In practical situations, reasonable initial approximations and possible constraints, imposed on the values of unknown parameters, may help discard some of the solutions. Under certain conditions this might allow to even use configurations "weaker" than those given above as minimal (as in the case with the configurations in the simulated tests to follow, in which only two directions of object lines are used !). The following examples will illustrate this point.

Two parallel lines perpendicular to a third provide 4 solutions for the rotations. When these directions are parallel to the X,Y,Z axes these solutions in fact are:

ω	φ	κ
ω	$\pi - \varphi$	$\pi + \kappa$
$-\omega$	$\pi + \varphi$	κ
$-\omega$	$-\varphi$	$\pi - \kappa$

It is evident that in most practical situations 3 of the triples can be discarded if the sensor orientation is only very roughly known.

On the other hand, the 8 solutions, obtained when the 3 lines are all orthogonal to each other, if again the directions are parallel to the X, Y, Z axes, are of the above form but for each of 2 triples $(\omega, \varphi, \kappa)_1$ and $(\omega, \varphi, \kappa)_2$. While the 3 solutions of each group of 4 could probably be discarded, the difference between the remaining solutions might well be small.

3.1.3. Accuracy assessment

3.1.3.1. Convergence rate

Numerous test runs showed that the algorithm is very robust against the approximate values for the rotation angles and can converge from quite far. The convergence rate is high regardless the presence of measurement noise and the wide diversity of the approximate values. More specifically in our simulation we have used approximate values differing up to 20^o from the true values, with and without the presence of measurement noise (up to the level of 21μm, max. absolute error). In all cases the algorithm converged correctly to the true values within at most 4 iteration loops. Thus,

within this range of initial values, no problems have been met, despite the fact that the object lines, which were used, defined only two directions in object space.

3.1.3.2. The role of geometry

It is apparent that the accuracy in the determination of the rotations depends upon the orientation and the relationship of the control lines. Therefore in order to study the role of the geometry we have simulated different line configurations according to the following scenario (Fig. 2).

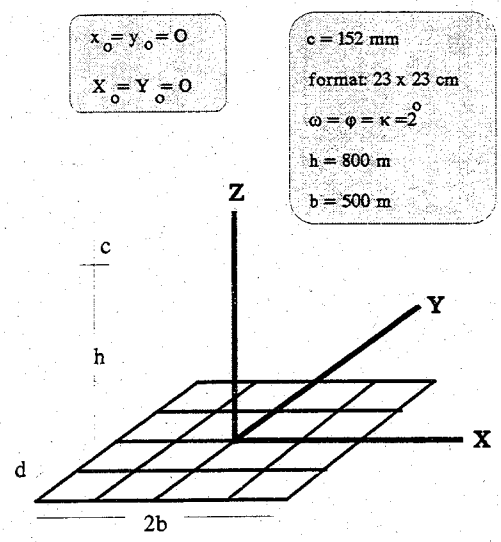

Figure 2: The simulated grid of points and the used ground coordinate system.

The assumption is that a grid of 5x5 points, with spacing d=250m, cover a ground area of 1km^2 and form a horizontal plane. The projection center is located above the center of the grid at flying height h=800m. The camera constant is assumed c=152mm and the image format is 23cm x 23cm. Simulated values for the rotation angle is $\omega=\varphi=\kappa=2^o$. The ground coordinate system is the one shown in Fig. 2 and with the above parameters the image coordinates of each of the 25 points have been calculated.

From these coordinates the best fitting lines (x/a + y/b + 1 = 0) to these points have been generated and their parameters (a and b) are assumed to be the original observations followed in Eq. (7) by a variance-covariance matrix as computed by the line fitting adjustment.

In order to form different configurations of the control lines we have chosen the 5 different patterns shown in Fig. 3 (Cases A to E). These patterns cover all the possible cases for a grid of points.

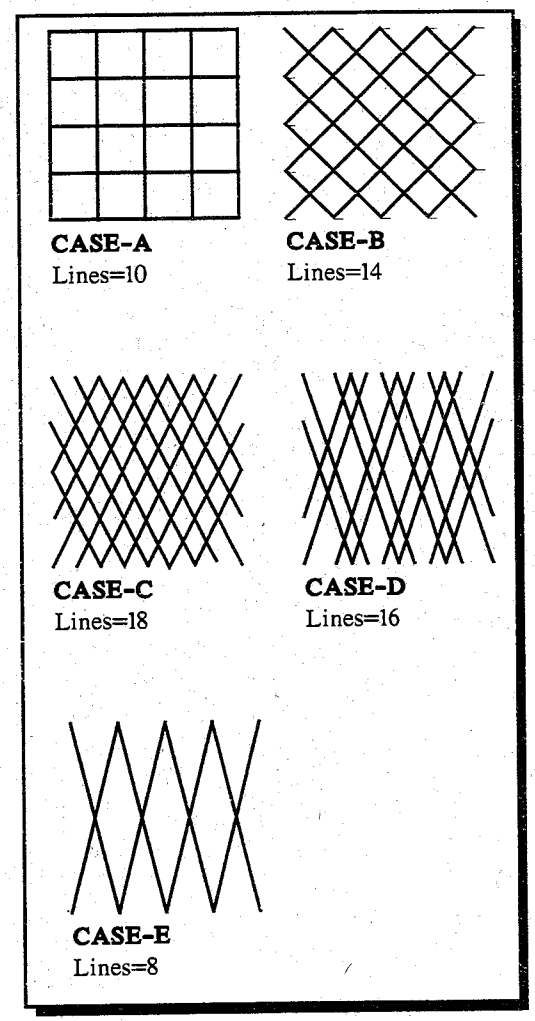

Figure 3: The 5 different simulated cases of control line patterns.

The evaluation of the role of the geometry is achieved through the evaluation of the co-factor matrix Q of the adjusted values (eq. 8).

$$Q = (A^T P A)^{-1} \tag{8}$$

where A is the design matrix of the adjustment and P the weight matrix of the measurements. The below shown values are the square roots of the diagonal elements of the Q matrix. The results are shown in Table 2 and Figure 4.

Table 2: Co-factor values of the angles ω,φ and κ for the five tested cases

	Case-A	Case-B	Case-C	Case-D	Case-E
$\sqrt{Q_w}$	0.0239	0.2750	0.2303	0.2055	0.2226
$\sqrt{Q_\varphi}$	0.0231	0.2749	0.4553	0.6068	0.8750
$\sqrt{Q_\kappa}$	0.0098	0.1166	0.1016	0.0879	0.0973

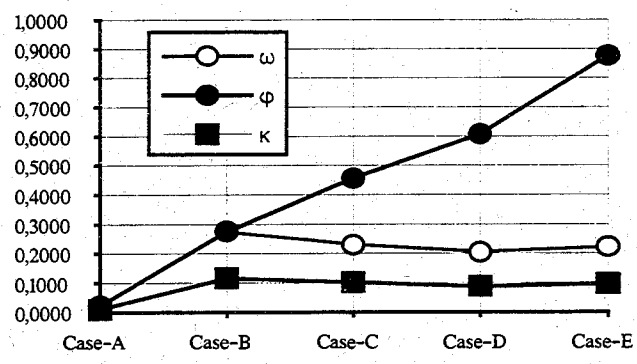

Figure 4: The computed values of the co-factor matrix Q for the rotation angles in the tested cases.

3.1.3.3. The role of number of lines

As we have seen 3 control lines is the minimum requirement for the determination of the rotational elements, avoiding the above mentioned critical situations. It is of course known that the more control lines are available the better the adjustment results are. However, it is important to study how these results are improved with the inclusion of additional lines. It is also important to know how this improvement proceeds in the presence of noise. Typically, this is an optimization problem, which should be solved as usual with analytic formulation. Here we confine ourselves to some simulation results.

Regarding the assumed number of control lines in the different cases studied so far, we formed the patterns 1,2 and 3 with minimum, medium and maximum control. Fig. 5 shows, for example, the different configurations in Case-B where the control lines assumed are bolded.

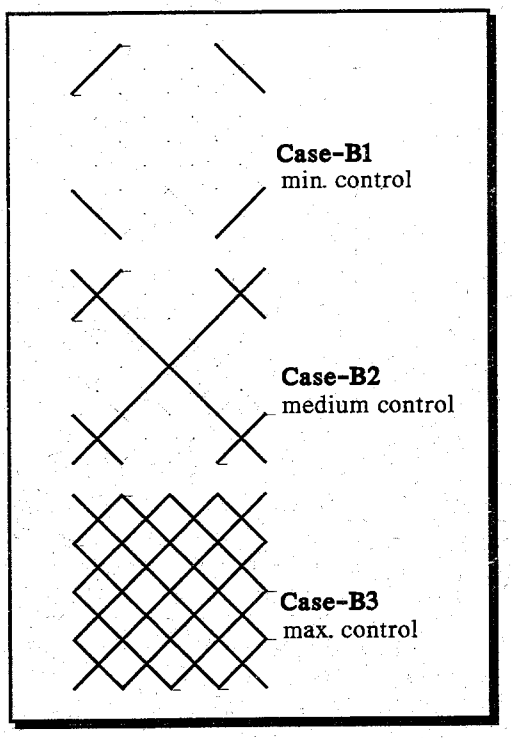

Figure 5: The formed minimum, medium and maximum control configurations for Case-B.

Besides running error-free data, we have also contaminated the measurements with noise of different level. These noisy measurements are been used through out our tests and worth more explanation here. The generated noise is assumed random and is according to the following scenario: In order to achieve results of practical importance we assumed that the lines can at least be extracted to sub-pixel accuracy (1/2 pixel) from the digital image. Assuming pixel sizes of 42μm and 21μm (corresponding to image resolution of 600dpi and 1200dpi respectively) we then set σ=21μm and σ=10μm as noise level.

Table 3: RMS values of the ω,φ,κ angles and the trace of their covariance matrix for all tested cases and for noise level of σ_o=10μm and σ_o=21μm.Values are in degrees x 10^{-3}

noise level	(°).10^{-3}	Case-A	Case-B	Case-C	Case-D	Case-E	**BUNDLE**
σo=10μm	**σω**	0.649	1.019	0.954	0.878	0.849	**0.393**
	σφ	0.655	1.018	1.905	2.629	3.381	**0.393**
	σκ	0.206	0.159	0.239	0.290	0.307	**0.768**
	trΣ	0.945	1.449	2.144	2.787	3.499	**0.948**
σo=21μm	**σω**	1.298	2.039	1.908	1.812	1.698	**0.786**
	σφ	1.311	2.036	3.809	5.423	6.765	**0.786**
	σκ	0.412	0.319	0.478	0.597	0.614	**1.535**
	trΣ	1.890	2.899	4.287	5.749	7.002	**1.895**

For comparison reasons the variance-covariance matrix of the adjusted rotational elements (Σ) has been calculated together with its trace (eq. 9 and 10). The values of trΣ are shown in Fig. 6 for Case-B. Similar figures have been obtained for all other case.

$$\Sigma = \sigma_o Q \tag{9}$$

$$tr\Sigma = \sqrt{\sigma_\omega^2 + \sigma_\varphi^2 + \sigma_\kappa^2} \tag{10}$$

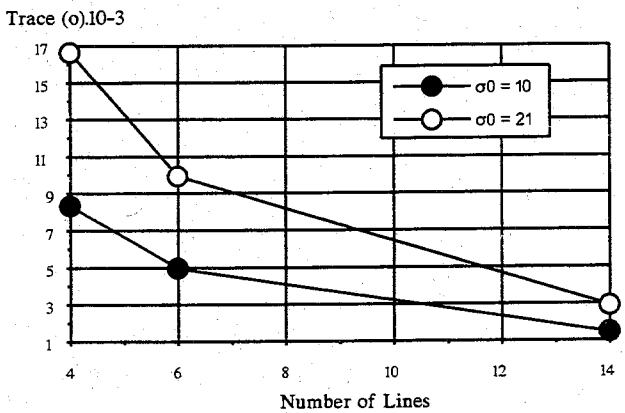

Figure 6: Values of trΣ for different number of control lines (see Fig. 5) and different level of measurement noise for Case-B.

The improvement of the accuracy is an exponential function of the number of control lines (n) regardless of the noise level. It is also clear, as expected, that this improve-

ment is more profound when the measurement noise is higher. Empirical functions of such an improvement are shown below:

$tr\Sigma \approx 60 \cdot N^{-1.4}$ for σ_o = 10μm and $tr\Sigma$ in $(^o).10^{-3}$

$tr\Sigma \approx 120 \cdot N^{-1.4}$ for σ_o = 21μm and $tr\Sigma$ in $(^o).10^{-3}$

3.1.3.4. Accuracy of rotational elements

In order to assess the accuracy of the attitude estimation, the RMS values for the rotational elements and the trace of the variance-covariance matrix for all tested cases and for the two noise levels are tabulated in Table 3 and shown in Figs. 8 and 9.

Also shown are the results of the regular resection adjustment for the above configuration of the 25 points. These results have been obtained assuming point measurements, and are shown here for comparison purposes.

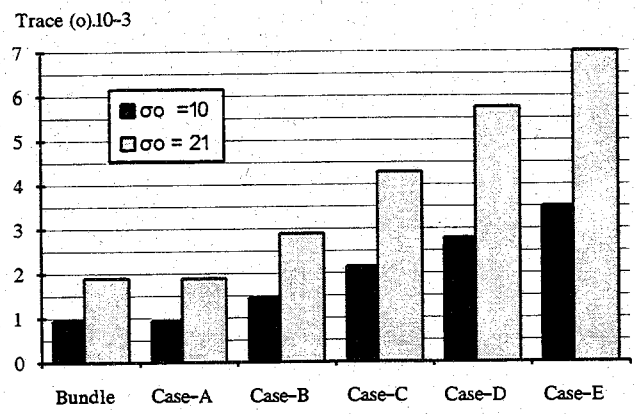

Figure 7: $tr\Sigma$ in all tested cases in comparison to that of regular bundle with point measurements.

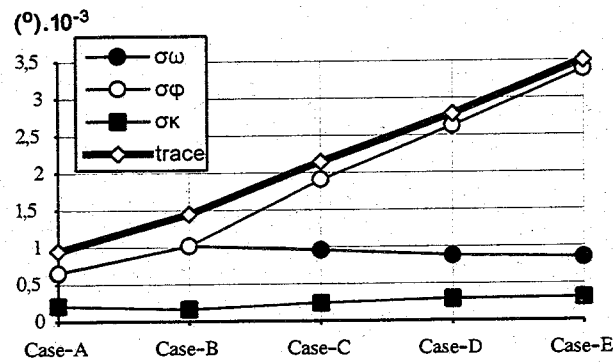

Figure 8: RMS values for the rotation angles and the $tr\Sigma$ for all tested cases for measurement noise of σ_o=10μm level.

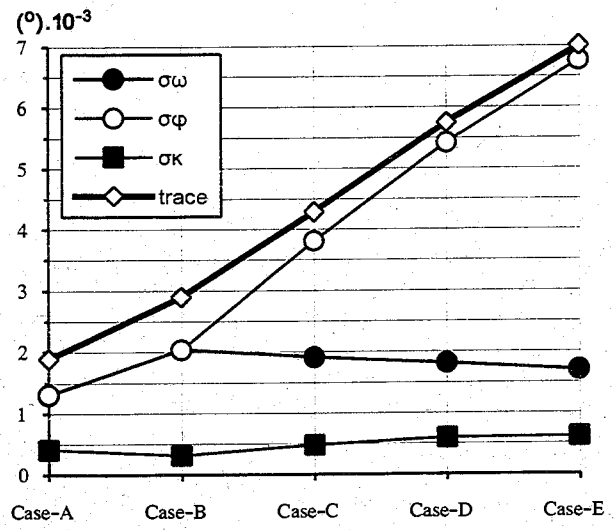

Figure 9: RMS values for the rotation angles and the trΣ for all tested cases for measurement noise of σ_o=21μm level.

The strength of the geometry of the orthogonal lines (Case-A) is evident and the compatible accuracies for the rotational elements for lines parallel to the axes (Case-A) is clear.

Compared to regular bundle approach, Fig. 7 shows clearly that the proposed approach provides equally accurate results when some basic precautions are respected (see also *Strunz, 1992* for similar conclusions). Needless to say that the quoted bundle configuration is quite strong and the obtained results are rarely met in practical situations.

3.2. Determination of sensor location

3.2.1. Critical configurations - Degeneracies

The location of the perspective center O (X_o, Y_o, Z_o) is geometrically determined as the intersection of the three projection planes E_1, E_2, and E_3 formed by three object lines L_1, L_2, and L_3, respectively; thus three lines known in object space is the minimal requirement. However, a degeneracy leading to an infinite number of solutions emerges when the three projection planes E_i have further points in common besides the projection center, i.e. when the determinant of the coefficients of the planes vanishes. This happens when :

- Lines L_i generating planes E_i are parallel to each other, i.e. they intersect at infinity. In this case the projection center O lies somewhere on a line parallel to three object lines L_i.
- Lines L_i have a common point of intersection. In this case O lies on the ray through this common point.

Both Mulawa (1989) and Strunz (1993) have pointed to the above two cases. However, a third case of degeneracy is to be found, namely :

- When the three lines L_i are skew to one another but there exist points T_i one on each of them, lying on the same ray passing through O. This configuration is to be seen in Fig. 10 below.

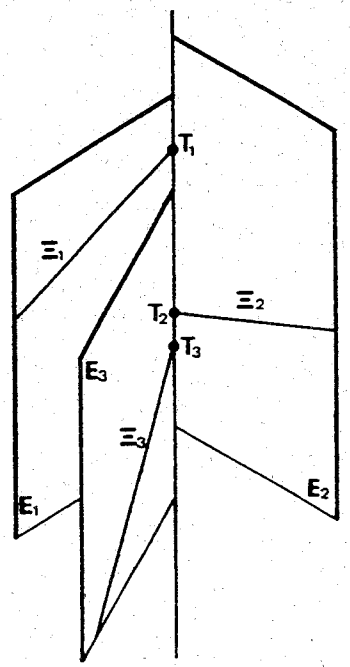

Figure 10: The three lines L_i are skew to one another but there exist points T_i one on each of them, lying on the same ray passing through O.

The above three critical cases can be summarized in one :

The location of the perspective center O cannot be determined when there exists a ray through O intersecting all object lines, including intersection at infinity.

And phrased otherwise : location of O is impossible when the lines intersect in object space and/or image space.

3.2.2. Minimum control requirements

The above degeneracy gives rise to an infinite number of solutions in the case of the generalized critical configuration mentioned above. In this case the problem is subject to indefiniteness. **With this exception, Three known lines in object space suffice for uniquely locating the image perspective center.**

4

RELATIVE ORIENTATION USING STRAIGHT LINE FEATURES

The typical photogrammetric problem of relative orientation consists in using as sole information at least 5 homologous points of a stereopair in order to determine a rotation matrix **R** and a translation vector **t** expressing the relative positions of the two images. The rank deficiency is accounted for by fixing the 7 parameters of similarity transformation (absolute orientation) by using an arbitrary scale and referring, for instance, to the system of the first image. The condition to be satisfied is that the homologous projection rays of the two images intersect. Shape and relative position of objects can be found simultaneously thereafter.

4.1. The case of the stereopair

Skewness is the "natural" relative position of homologous rays of stereopair with arbitrary relative orientation, i.e. intersection of rays imposes an actual constraint on relative orientation. It is self-evident that this is not so when homologous lines rather than points are employed : the **two projection planes defined by corresponding image lines** on the two images, and in fact all pairs of corresponding projection planes, **will always intersect** (when not parallel or coincident) irrespective of the particular relative orientation. The intersection of planes that imposes no constraint on orientation. **The problem is inherently (i.e. geometrically) insolvable regardless of the number of image lines correspondences used.**

Even the use of known angular relations among space lines does not provide a full answer to the problem of relative orientation of the stereopair. Such angular information may in fact allow recovery of the rotations (as it is also the case with the determination of the rotational elements of the exterior orientation). If the rotations are thus established, however, the projections centers of the images can still slide freely without affecting the directions of the intersections of the corresponding projection planes. since these planes will remain parallel to their former positions. **Thus angular relations among object lines do not suffice for the recovery of the translational parameters of relative orientation**. It seems that the problem might be solved if also positional relations, e.g. intersections, equal distances etc., are available.

4.2. The case of image triples

Contrary to the above, three planes generally intersect in a point : the requirement of a common line of intersection thus poses an actual constraint on relative orientation. The equivalent of the 5 homologous points in a stereopair is 6 lines in triple of images allowing the recovery of the 11 elements of relative orientation, with one redundancy.

More generally, the minimal requirements for the relative orientation of n images are m = 5 + 6(n-2) lines.

As indicated above, translations of the perspective centers cause projection plane intersections to move parallel to themselves. In this sense, recovery of **R** and **t** may well be separated in a two-step procedure. The condition for the recovery of the rotations is that homologous projection planes intersect by two in parallel lines (see also Fig. 11). That lines have a point in common is the condition for recovering the linear parameters. At the other end, relative orientation may simultaneously proceed with object reconstruction (in the normalized coordinate system, i.e. the model system) in a unified procedure.

The problem of relative orientation using straight line features has been initially investigated by Sebastian Finsterwalder, who has given the basic equations for the rotational parameters (*Finsterwalder, 1937*). Several decades later the very same problem was first re-encountered in computer vision. In fact relative orientation and

object reconstruction are tasks equivalent to those of "motion" (moving camera or rigidly moving scene) and "structure" from image sequences. Also in this respect, photogrammetry has much to benefit from research in computer vision where, in the last decade, several algorithms for determining motion have been developed (*Liu and Huang, 1988; Mitiche and Habelrih, 1989; Huang 1990; Weng et. al., 1992, 1993; Strunz, 1993, Navab, 1993*).

4.3. Determination of relative orientation parameters

4.3.1. Rotational parameters

Referring to Fig. 11, let the perspective centers of an image triple be O_1, O_2, O_3 and consider homologous image lines l_i i=1,2,3 which are represented in their intercept form $x/a_i + y/b_i + 1 = 0$, whereby x, y refer to the particular image coordinate system of each image. If by ε_i the projection planes of lines l_i are denoted, the normal vectors $\mathbf{j}_i$ of these planes can be written in the following form (see also section 2):

$$\mathbf{j}^T = [\, -c\,b \quad , \quad -c\,a \quad , \quad a\,b + b\,x_o + a\,y_o \,]$$

in which c, x_o, y_o are the interior orientation parameters of the respective image. Let $\mathbf{R}_i$, $\mathbf{t}_i$ be the rotation matrices and the translation vectors, respectively, which describe the orientation of the three images in the normalized coordinate system XYZ of the first image (i.e. $\mathbf{R}_i = \mathbf{I}$ and $\mathbf{t}_i = 0$). In this system, the equations of the three homologous projection planes ε_i can be expressed in the form :

$$\mathbf{j}^T \mathbf{R}\ (\mathbf{X} + \mathbf{t}) = 0 \qquad (11)$$

in which $\mathbf{X}^T = [\, X\ Y\ Z \,]$ is the coordinate vector of a point of the respective projection plane ε_i. If $\boldsymbol{\delta}^T = [\, L\ M\ N \,]$ is the direction vector of model line L, the projection planes ε_i are parallel with it when for all three of them holds :e respective cthehthtttt

$$\mathbf{j}^T \mathbf{R}\ \boldsymbol{\delta} = 0 \qquad (12)$$

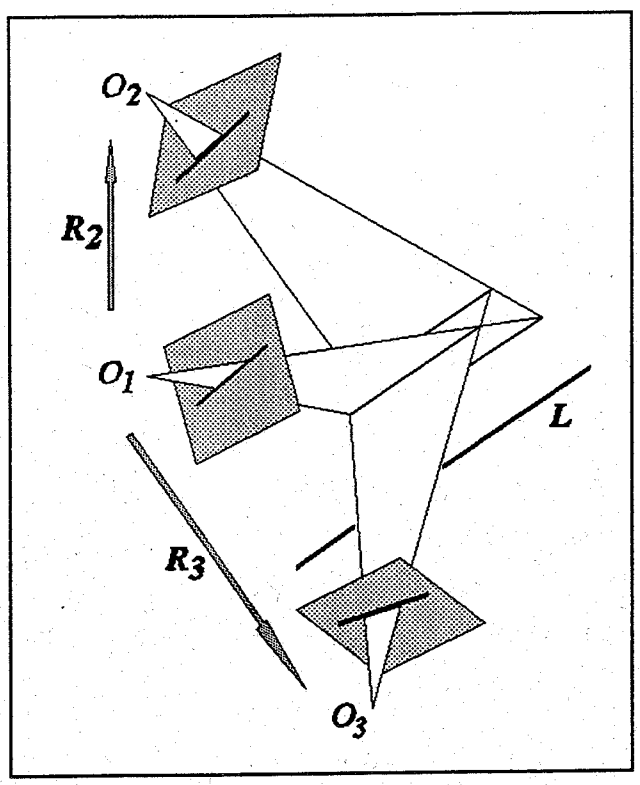

Figure 11: Basic geometry of (rotational) relative orientation of image triples using straight lines. The three homologous projective planes intersect in the model line ***L***.

The homogeneous system of three equations in L, M, N expressed by eq. (12) has non-trivial solutions when the determinant of its coefficients vanishes. This is the condition that the three projective planes intersect in lines parallel to model line ***L*** (Fig. 11). Thus expression of the normal vector of each of the three projection planes ε_i through the directional coefficients of the same plane in the model system as $\mathbf{j}^T \mathbf{R} = [\, u\ v\ w\,]$ and introduction of these expressions in eq. (12) will finally yield :

$$u_1 (v_2 w_3 - w_2 v_3) + v_1 (w_2 u_3 - u_2 w_3) + w_1 (u_2 v_3 - v_2 u_3) = 0 \qquad (13)$$

The condition equation connects the 6 relative image rotations with the parameters a_i, b_i of the image line l_i. These latter parameters are regarded as the observables with variance-covariance matrices known from the image line fitting process. 6 triples of homologous image lines suffice for the determination of the rotations of the two images with respect to the first. These are conventionally denoted by $(\omega, \varphi, \kappa)_2$, $(\omega, \varphi, \kappa)_3$. Since the condition equation is non-linear initial approximations are required; they can be obtained by partial space resection if the directions of three model lines are only roughly known (see also section 3).

Finally, the directions $\boldsymbol{\delta}$ of the employed model lines L can be determined from eq. (12) using an appropriate constraint (see eq. (1a), (1b)) to express the fact that only two of the L, M, N direction numbers are independent.

4.3.2. Translational parameters

Eq. (13) is not sufficient for the condition that the homologous projection planes have a common line of intersection, i.e. line L. Therefore, besides eq. (13) a further condition is needed to make all three planes have a point in common for which eq. (11) holds. To this end the point of line closest to the origin of the model coordinate system may be considered, say point $\mathbf{X}_c^T = [\, \mathbf{X}_c\,,\ \mathbf{Y}_c\,,\ \mathbf{Z}_c\,]$. Hence, this would satisfy the condition :

$$\mathbf{X}_c^T \boldsymbol{\delta} = 0$$

This equation can be combined with eq. (11), thus resulting in a condition linear in the translational parameters of the other two images relative to the system of the first, which are conventionally denoted by $(bx, by, bz)_2$ and $(bx, by, bz)_3$.

A considerably simpler solution, however, can be obtained if one of the points of intersection of model line L with the three planes of the coordinate system is chose. If, for instance, $L^2 > (M^2, N^2)$ point $\mathbf{X}_t = [\, 0\,,\ Y\,,\ Z\,]$ can be used. If

$$d_i = \mathbf{j}_i^T \mathbf{R}_i \mathbf{t}_i \qquad , i = 2, 3$$

in this case eq. (11) yields :

$$d_2 (v_1w_3 - w_1v_3) - d_3 (v_1w_2 - w_1v_2) = 0 \qquad (14)$$

From eq. (14) it is obvious that the translations $\mathbf{t}_2$, $\mathbf{t}_3$ cannot be recovered independently. A constraint has to be imposed on them to fix the scale, for instance, by giving an arbitrary value to one of the $|\mathbf{t}_2|$, $|\mathbf{t}_3|$ or to one of the elements $\mathbf{t}_2$, $\mathbf{t}_3$. Here, this latter approach has been adopted by fixing the bx_2 basis component.

Thus, eq. (14) allows the recovery of the two translation vectors when 5 line correspondences in an image triple are known. Here again, the two image line

parameters with their variance-covariance matrices are used as observations. This equation is linear in the translations. From eq. (11) and the imposed constraint for the reference point of the line, its coordinates can be recovered.

4.4. Critical configurations - Degeneracies

With a minimum of 6 lines appearing on 3 images and a total of 11 independent parameters, the photogrammetric problem of relative orientation using lines is significantly more complex to analyze theoretically than the corresponding one with points. It is not known, for example, how many solutions there may be when the minimum of six lines are used (*Huang, 1990; Navab, 1993; Weng et.al., 1993*); *Faugeras (1993)*, however, expects the solution to be in fact unique due to the one redundancy available. The important theoretical studies of *Buchanan (1992(a), (b))* have revealed critical line sets beating all available algorithms by leading to a multiplicity of solutions, a point which has been further elaborated upon in a framework more familiar to photogrammetrists (*Navab, 1993; Navab et.al., 1993*). Also the remarks of *Faugeras (1993)* on this subject are very illuminating indeed.

Finsterwalder (1941) has early identified two cases of indefiniteness when **all three perspective centers are collinear** :

- *An object line coplanar with the line of the perspective centers, whence the homologous projection planes coincide.*

- *Object lines are coplanar.*

Both cases, and mainly the second one (flat terrain), are of particular interest to aerial photogrammetry where images of the same strip are usually used. Based on this, Strunz (1993) has concluded that the method is not suitable for aerial imagery.

Initiated by the need for a guide for practical situations of terrestrial applications, the simulations carried out here have encountered several other, relatively simple, configurations apparently leading to lack of solutions. These simulations were based on a simple object involving three planes, two perpendicular to each other (a cube cut across one of its diagonal planes of symmetry). A total of 52 lines were created defining several directions in space. The described algorithms were used with no

perturbations of image line parameters and minimal line control. A distinction was made between total lack of solution and recovery of rotational elements only. Configurations were checked with reasonable initial approximations as well as the true values, and were chosen by both geometric reasoning and guessing. The patterns studied here can be summarized as : special configurations of lines with both random and particular position and orientation relative to the perspective centers while the latter were either all collinear or randomly distributed. Once a conclusion appeared as likely, it was checked with otherwise totally random configurations, i.e. retaining only the assumed source of degeneracy. The following conclusions are thus based on a total of more than 300 simulations. Examples of simple geometries not giving solution for particular perspective center distributions are given in Fig. 12.

A distinction has been made here between indefiniteness and multiplicity of solutions. A pattern was considered to be "degenerate" either if it led to no solution at all (singularity) or if it gave rise to convergence only to solutions other than the true one. Cases treated here as "non-degenerate" may, obviously, give multiple solutions (and several actually did). Needless to stress that the conclusions to follow are only provisional, founded basically on simulated examples. A certain consistency they display, however, indicates that they are likely to be valid.

Additionally to the two cases cited above, **collinearity of the three perspective centers does not allow solution with** :

- *Five coplanar object lines, one random.* The rotational parameters can separately recovered.

Thus, collinearity of all perspective centers results in the restriction of at most 4 lines lying on the same plane.

Four, out of six, coplanar lines generally allow solution. The degenerate cases encountered are as follows :

- *Four lines on plane π, two lines perpendicular to π.* The rotational elements are not recovered separately, either (see Fig. 12a).

- *Four lines on plane π, two lines intersecting on π, intersection at infinity included.* Rotations can be solved for separately (see Figs. 2b, 2c).

Generally, **no solution is found in the following case** :

- *Six lines on planes π and π', with the latter intersecting in a line coplanar with the line defined by the three perspective centers.* The rotations can be found separately. (For instance, the configuration of Fig. 2d provides no solution with perspective centers lying on the vertical line).

Further, **for lines lying in threes on two planes,** the following degenerate cases were encountered :

- *Two line triples on planes π and π', each three having the same common point, intersection at infinity included.* Here, rotations were recovered separately only when both triples did not consist of parallel lines (see Figs. 2e, 2f; cf. Fig. 2g).

- *Two line triples on planes π and π' with the one triple intersecting on the intersection of π and π', intersection at infinity included.* Here again, rotations could not be solved for in the case of parallelism (see Figs. 2g, 2h, 2i).

Finally, two more cases were met, in which no solution was possible for collinear perspective centers, namely :

- *Lines on planes π and π', with π parallel and π' perpendicular to the line defined by the perspective centers.* The rotational parameters are not found separately (eg. the configurations of Fig. 2j with perspective centers on a vertical line).
- *Lines on three planes intersecting in a line coplanar with that defined by the perspective centers.* Here, it is possible to solve separately for the rotational parameters.

The only case met in which in which a line configuration would deny solution, regardless of its position and orientation with respect to the **randomly positioned (not collinear) perspective centers**, was the following :

- *Five parallel lines, one random.*

  A separate recovery of rotations is not possible either.

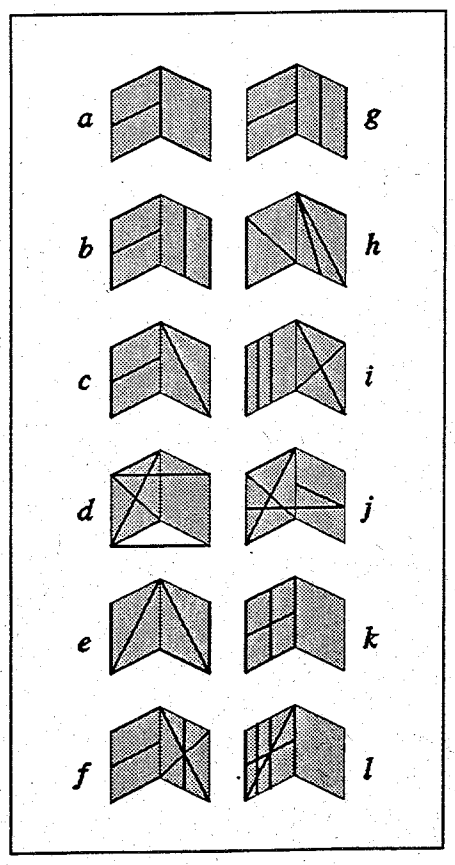

Figure 12: Examples of simple line distributions not allowing solutions for particular configurations.

However, certain interesting intermediate cases have been also identified with non-collinear perspective centers. Thus, no solution exists for :

- *Coplanar lines in two directions (either 4 + 2 or 3 + 3, since 5 + 1 has been just rejected) with the one direction parallel to the :*
  - *plane defined by the perspective centers;*
  - *line defined by two of the perspective centers.* In this case the rotations are not found separately. (E.g. the configuration of Fig. 2k for perspective centers lying on a plane parallel to the diagonal plane of the cube or two perspective centers lying on a vertical or a horizontal line).

- *Coplanar lines, of which four are parallel having either of the above two particular relations to the perspective centers.* Rotations again cannot be recovered separately (see Fig. 2l).

These are the basic provisional conclusions of this study regarding non-existence of solution in relative orientation using straight line correspondences. It is evident that

many simple line configurations, which would seem suitable for this task in terrestrial applications, in fact are not. Space does not allow to present other, equally simple patterns, which would allow solution. Instead indicative results using simulated data for an elementary line configuration are given next.

4.5. Simulated example

Photography of a house corner was simulated considering a camera of middle format and wide-angle lens. Imaging distance is 6m and the object's dimensions are about 6x6x6 m^3. The cameras of two convergent images are placed at approximately 1 : 5 of the imaging distance on either sides of the central camera and are not very far from been collinear differing from it by 20cm in height and 50cm in depth. The seven lines shown in Fig. 13 were used.

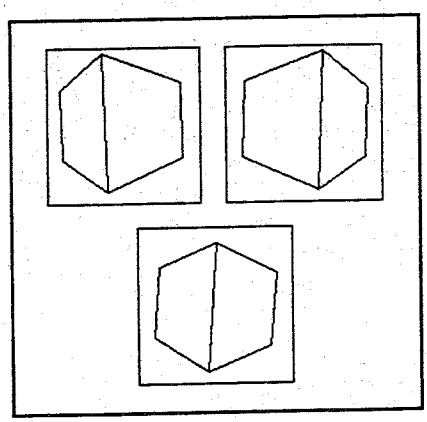

Figure 13: The three simulated images used in relative orientation with respect to the lower image.

Edge points on the fictitious image lines were densely sampled, perturbed with σ = 12μm and subject to line fitting resulting in the a, b parameters and their variance-covariance matrix. The results of the above described algorithm, in which parameter bx_2 was kept fixed, are seen in Table 4.

The differences from the correct values are compatible with the standard errors. These results are comparable with the solution obtained using points. Finally, regarding object reconstruction the problem of accessing the accuracy of the estimated lines will not be discussed here (refer eg. to *Wenzhong and Temphli (1994)* for an interesting discussion. It may be simply mentioned that the orthogonalities between lines have been recovered with an RMS of 0°.003, while the distance between lines with an RMS

been recovered with an RMS of 0°.003, while the distance between lines with an RMS of 1.6cm.

Table 4: Simulation results of relative orientation parameters using 7 object lines.

	Estimated values of Parameters	Differences from correct values	Standard errors of parameters
ω_2 (°)	0.284	-0.004	0.028
φ_2 (°)	4.012	-0.022	0.035
κ_2 (°)	-5.974	-0.035	0.038
ω_3 (°)	-0.429	0.009	0.035
φ_3 (°)	-6.022	0.037	0.044
κ_3 (°)	-2.067	0.045	0.049
bx_2 (m)	*(1.093)*		
by_2 (m)	-0.267	-0.001	0.004
bz_2 (m)	-0.483	-0.001	0.002
bx_3 (m)	-1.402	0.001	0.002
by_3 (m)	-0.093	-0.001	0.005
bz_3 (m)	-0.526	-0.002	0.002

5

A PRACTICAL EXAMPLE

5.1. The Object

The test object chosen is one of the Otto Wagner's Stadtbahn Station buildings on the Karlplatz in Vienna, Austria (Fig. 14). Its dimensions are 15x8x10m^3. A 6-station surveying network has been established around the building and the polar coordinates of 44 non-signalized (but well defined in majority) control points have been measured. After the adjustment of the surveying measurements, the local cartesian coordinates of the control points have been determined with an rms values of 2mm. These points cover all four exterior facades. Based on these control points and the available imagery, a coarse CAD-model (CAD-sketch) has been obtained through a regular bundle adjustment. This coarse model contains major structure lines of the building, to be used in the following analysis as *"control lines"*. Furthermore, it helps both in the detection of the corresponding image lines and in the correspondance of these detected lines in the different images, as it is explained later on.

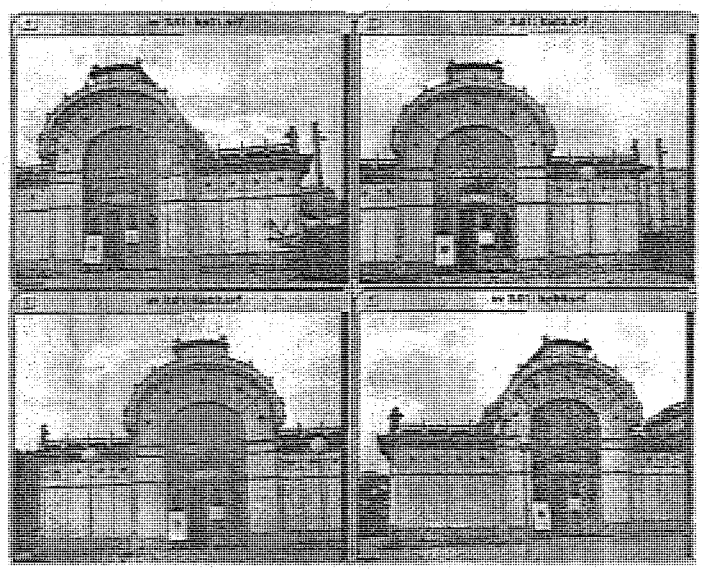

Figure 14: Otto Wagner's Pavillion. The four images used in the test.

5.2. Image acquisition

In Digital Photogrammetry images are captured either with film-based cameras and subsequent digitization, or with cameras with solid-state sensors. Devices of the latter type can be standard solid-state cameras with a video recorder or a computer with a framegrabber, still video cameras, video cameras, and several types of high resolution CCD cameras. Conventional film-based cameras still provide an unsurpassed photographic photographic resolution, but the film must be developed and digitized before its data become available for photogrammetric processing. Solid-state cameras, on the other hand, provide immediate access to the image data, with the drawback of a coarser resolution. Today a variety of solid-state imaging systems, ranging from inexpensive camcorders to specialized high resolution systems, is available at the market (Luhmann, 1992).

Although camcorders are not intented for photogrammetric use, they excibit many useful characteristics. They are inexpensive and widely used for other pursposes as well, they are portable and free-hand, they need no special equipment, they offer the ability of on-site quality control. Furthermore they provide a very inexpensive means for storage of huge amount of data in video tapes. Their major disadvantage is their low resolution, which poses some limitation on the number of measurable details, and of course their geometrical instability. However, previous studies (Streilein, 1994, Streilein, et. al., 1993) have shown that with proper calibration sufficient accuracy for architectural tasks can be otained under normal practical situations.

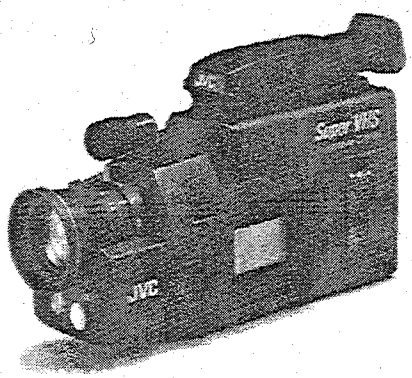

Figure 15: The JVC GR-S77E camcorder.

The JVC GR-S77E Camcorder is an inexpensive consumer product (Fig. 15). It is a free-hand portable camera and the on-site control for the acquired imagery is achieved by the internal monitor. It incorporates a 1/2" (6.4mm x 4.8mm) color sensor with ca.

420.000 sensor elements. The imagery can be directly transmitted to a frame grabber or recorded on a S-VHS C tape. The digitized images have a size of 728x568 pixel, which results in a pixel spacing of 8.5μm in the horizontal and 8.3μm in the vertical direction.

The whole building was covered by 24 images taken by the JVC GR-S77E camcorder. However, for the purpose of this test only 4 photographs corresponding to the first facade have been used (see Fig. 14).

5.3. Extraction and correspondance of straight lines

The DIPAD system (Digital Photogrammetry and Architectural Design) devoped in ETH (Streilein, 1994) has been used in this test. DIPAD consists of a Digital Photogrammetric Station (DIPS, (Gruen and Beyer, 1990)) and a Computer Aided Architectural Design (CAAD) module and allows for automatic and semi-automatic measurement of image coordinates (template matching (Gruen, 1985)), or manual measurements.

The mentioned before CAD-sketch roughly (using initial approximate values for e.o.) transformed into image space is used as starting point for the automating feature extraction algorithm. This algorithm is based on local gradient operators to determine local intensity variations in the image signal. It is based on the assumption that discontinuities or rapid changes in the intensity of the image signal often occur at the physical extent of objects within the image. The localization of an edge in the image domain is equivalent to finding the maximum of the first partial derivatives (gradients) of the image intensity function. Gradients for the discrete image function are approximated by filter operators in orthogonal directions. In this algorithm, a row gradient $g_r(j,k)$ and a column gradient $g_c(j,k)$ are determined by the convolution of the image signal with the Sobel operators ∇r and ∇c (eg. 15). The following convolution kernels are used:

$$\nabla r = \frac{1}{4}\begin{bmatrix} -1 & 0 & 1 \\ -2 & 0 & 2 \\ -1 & 0 & 1 \end{bmatrix} \qquad \nabla c = \frac{1}{4}\begin{bmatrix} 1 & 2 & 1 \\ 0 & 0 & 0 \\ -1 & -2 & -1 \end{bmatrix} \tag{15}$$

Every pixel is assigned a gradient values (see Fig. 16) which is a vector containing a magnitude G(j,k) and a direction Θ(j,k) :

$$G(j,k) = (g_r(j,k)^2 + g_c(j,k)^2)^{1/2} \qquad \Theta(j,k) = \arctan\left(g_r(j,k) / g_c(j,k)\right)$$

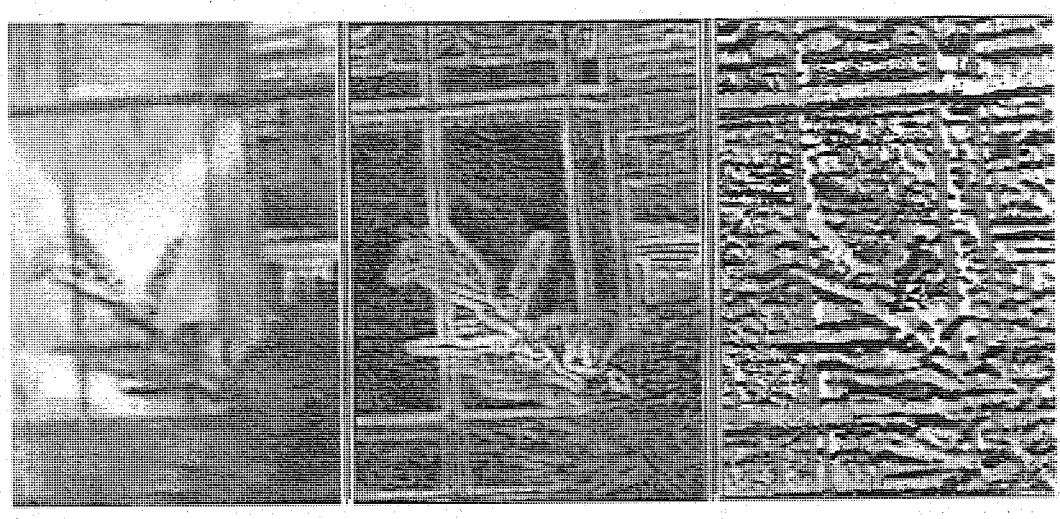

Figure 16: Gradient values derived by the Sobel operator. The original image is shown at the left. Magnitude of the gradient is shown at the middle. Direction of the gradient is shown at the right.

The position of the edge is then determined with subpixel precision by fitting a second-order polynomial in the direction of the gradient. The maximum point of the fitting curve corresponds to the subpixel position of the edge (see Fig. 17). The covariance matrix of the estimated polynomial parameters represents the accuracy of the edge point.

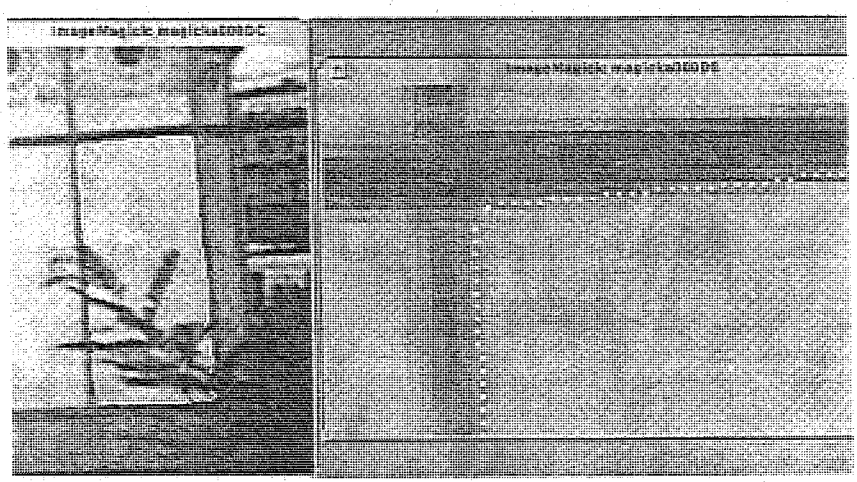

Figure 17: Zoom of the extracted image edge points at subpixel precision.

At the end of this process, a list of single edge points with subpixel precision is obtained. All edge points belonging to the same edge are then used to determine the edge parameters. The underlying edge model used in this test is a straight line. The observation values are given by the subpixel position of each edge point and its weight is proportional to the precision of this position. The parameters for the image straight line are determined by a Least Squares Estimation and their covariance matrix represents the accuracy of the extracted straight line.

Besides the precision of the detected edge, another important aspect for feature extraction is the significance of the detected structures. In real world problems typically occur due to occlusion, illumination effects (e.g. shadow edges), feature fading into background, or varying background. In order to handle such cases and to exclude insignificant structures, the algorithm rejects all edge points, from the list of points contributing to the entire edge, which do not fulfil the following two criteria :

- *The orientation of the gradient shound not deviate more than a user defined threshold from the orientation of the entire edge.*
- *The magnitude of the gradient should be higher than a user defined threshold.*

An example of the performance of these criteria can be seen in Fig. 18. The occluding structure of the bush at the foreground does not disturb the estimation of the straight lines at the background.

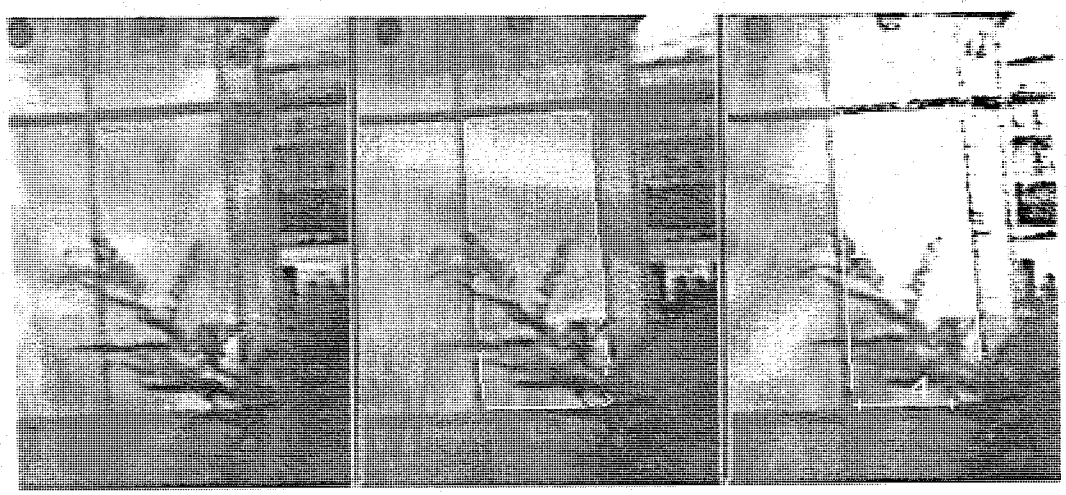

Figure 18: Example of the feature extraction algorithm.

Figure 19: Straight line extraction. *Upper* image shows the 20 extracted lines used for the determination of e.o. elements. The same lines (provided they appear) have been used in all four images. *Lower* image shows the 10 control points also used for the e.o. determination, for compariison reasons.

5.4. Determination of exterior orientation

From all the automatically extracted lines only 20 of them have been chosen to be used as "control lines" (Fig. 19) for the determination of the exterior orientation of the four images. These 20 lines have been chosen regarding mainly their geometry. Unfortunately not all of them appear in all four images. Therefore from these 20 lines, only those appearing in every image have been actually used.

The accuracy of their extraction has been estimated to 1cm level in planimetry (on the facade) and 2.5cm in height (perpendicular to the facade). Having in mind that the average scale of the four images is about 1:2,000 and the pixel size about 8.5μm, the extraction accuracy is approximately the pixel size (2,000x8.5μm=1.7cm on the ground).

Additionally, for checking purposes, 10 of the available control points (Fig. 19) have been used also for the detemination of the e.o., according to the regular photogrammetric practice.

In the following tables the determination of the e.o. using only the control points (Table 5) or only the control lines (Table 6) is shown.

Table 5: Exterior orientation using N control points

Photo	ω (°)	φ (°)	κ (°)	X_o (m)	Y_o (m)	Z_o (m)	
	σ_ω	σ_φ	σ_κ	σ_{X_o}	σ_{Y_o}	σ_{Z_o}	σ_o (μm)
1	9.198	11.914	−4.236	20.398	2.887	22.375	
N = 10	±0.430	±0.389	±0.092	±0.145	±0.163	±0.093	8
2	7.374	−9.108	−0.912	11.535	3.706	23.526	
N = 10	±0.931	±0.522	±0.108	±0.216	±0.380	±0.059	11
3	6.978	0.252	−2.380	12.106	3.798	23.734	
N = 10	±0.676	±0.395	±0.081	±0.165	±0.277	±0.039	9
4	6.976	−20.564	0.932	2.831	3.693	22.996	
N = 10	±0.616	±0.460	±0.134	± 0.175	±0.238	±0.115	10

Table 6: Exterior orientation using N control lines

Photo	ω (°)	φ (°)	κ (°)	X_o (m)	Y_o (m)	Z_o (m)	
	σ_ω	σ_φ	σ_κ	σ_{X_o}	σ_{Y_o}	σ_{Z_o}	σ_o
1	9.080	12.177	−4.381	20.491	2.907	22.299	
N = 14	±0.178	±0.195	±0.063	±0.071	±0.069	±0.055	1. 5
2	8.891	−9.054	−1.098	11.580	3.022	23.347	
N = 13	±0.739	±0.840	±0.099	±0.339	±0.298	±0.119	2.9
3	10.837	0.721	−2.486	12.325	2.170	23.665	
N = 13	±0.421	±0.454	±0.083	±0.191	±0.182	±0.042	2.5
4	7.320	−20.828	1.358	2.754	3.553	22.829	
N = 11	±0.904	±0.564	±0.166	± 0.211	±0.352	±0.165	2.4

From the above results it is obvious that the same parameters differ much in the two cases. Such differences are profound especially in Photo #3 ($\Delta\omega \approx 4°$ και $\Delta Y_o \approx 1.6$m). However, the high correlation between such parameters is very much noticable (Table 7).

Table 7: Correllation coefficients for e.o. elements of Photo #3.

E.o. using points							**E.o. using lines**					
ω	*φ*	*κ*	*Xo*	*Yo*	*Zo*		*ω*	*φ*	*κ*	*Xo*	*Yo*	*Zo*
1.000	0.216	−0.013	0.214	**-1.000**	−0.365	ω	1.000	−0.629	−0.592	−0.608	***-0.999***	0.351
	1.000	−0.095	**0.999**	−0.210	−0.471	φ		1.000	−0.153	***0.999***	0.642	−0.716
		1.000	−0.104	0.017	0.047	κ			1.000	−0.182	0.583	0.206
			1.000	−0.208	−0.464	Xo				1.000	0.620	−0.690
				1.000	0.355	Yo					1.000	−0.377
					1.000	Zo						1.000

This fact is not exceptional when the control points do not cover adequately the whole image format. In such cases, high correlations between the pairs $[\omega, Y_o]$ and $[\varphi, X_o]$ can be observed. In our case for the first pair the correlation was $-1 < \rho \leq -0.995$ (in the case of points) and $-0.999 \leq \rho \leq -0.995$ (in the case of lines). Regarding the second pair of parameters, the correlations were $1 > \rho \geq 0.997$ and $1 > \rho \geq 0.991$ respectively. It should be also noticed that Z_o is correlated (correlation $\rho \leq -0.85$) to φ

and X_o in the three of the four images (except Photo #3). *Therefore, it is clear that since the e.o. parameters are correlated, they should be faced as a group and they can not be compared individualy.*

In order to properly compare the results from bundle adjustment (using points) to those using lines, the following strategy has been followed: A regular grid of 12×6 = 72 image points x, y (Fig. 20) has been back projected on the facade (Z = 0), through the collinearity equations:

$$X = F_X(x,y,c;\ \omega,\varphi,\kappa,X_o,Y_o,Z_o;\ Z) \qquad Y = F_Y(x,y,c;\ \omega,\varphi,\kappa,X_o,Y_o,Z_o;\ Z)$$

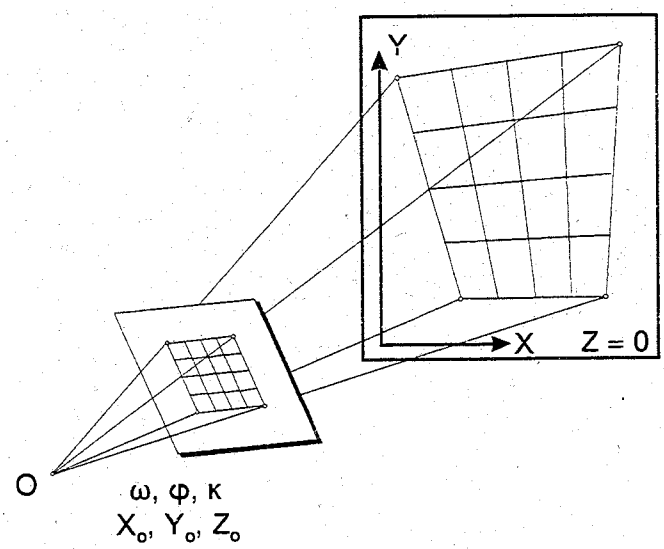

Figure 20: A sythetic regular grid of 72 image points have been projected back to the object assuming known e.o.

For all grid nodes the object space coordinates have been computed twice. First, using the e.o. parameters computed through points (X_P, Y_P, 0). Second, using the e.o. parameters computed through lines (X_L, Y_L, 0). The comparison of the two projected grids of the N=72 points

$$s_X = \sqrt{\frac{\sum (X_P - X_L)^2}{N}} \qquad s_Y = \sqrt{\frac{\sum (Y_P - Y_L)^2}{N}}$$

shows how well the two group of e.o. parameters "fit" the image to the object space. The results are shown below (Table 8).

Table 8: RMS (s) and Average (μ) differences in object space coordinates obtained through the two procedures.

	s_X (cm)	s_Y (cm)	μ_X (cm)	μ_Y (cm)
Photo #1	0.7	2.7	–0.2	2.5
Photo #2	2.5	2.7	–0.2	2.4
Photo #3	2.3	2.5	–1.4	2.2
Photo #4	1.4	3.0	–0.2	1.2
Average s	1.9	2.7		

From the above results it is obvious that the accuracies depend mainly on the geometries of the used lines in the specific images. At average, the computed rms differnces are $s \leq 3$ cm, which is according to the expectations, we stated in the beginning.

Therefore, safely one can state that *the determination of the e.o. using lines is compatible accuracywise with the e.o. determined by the regular photogrammetric procedures using point data.*

6

CONCLUDING REMARKS

Although photogrammetric procedures are based on observations of points on images, it is apparent that points are entities of weak description power. In the man-made environment, objects are certainly described best by other features such as straight lines, arcs, circles, ellipses or other mostly analytically describable functions (e.g. higher order polynomials, splines, etc.). In natural environment, point has never existed not even as an entity; it is rather a mathematical abstraction like the "point mass", the "white noise" and so on, which helps in describing natural phenomena, like for instance breaklines, possibly even not in the best way.

This weakness of point-based procedures is often apparent in photogrammetric tasks, where although enough features exist, the number, the position, the distribution, or the quality of intersection points may result to ill-conditioned solutions. This is especially important if the aim is to automate the photogrammetric procedures, where certainly the desire is that no human inspection or interference during the process should be involved.

Of course there are difficulties and limitations with this approach too. One could argue that there may be not enough straight lines, not of sufficient length, or not in suitable locations in the different images. It is true that in certain situations that may be the case, as for instance, in satellite images. But even in this case, what actually is the alternative procedure? To identify control points as well defined junctions of roads or other linear features and to make sure that these points are also well identified (or even exist) in the next images, and are properly located. It is obvious, therefore, that at least Line Photogrammetry does not impose further limitations. On the contrary, instead of identifying points (with all the accuracy degradation this may involve) generic

line features are used. Furthermore, even if only a part of this line appears in the next images, this is sufficient to proceed on. And most importantly, Line Photogrammetry is a more natural model for non-frame sensor, like the satellite sensors.

In this work we have only dealt with the use of straight linear features. Certainly, other higher order features like arcs, circles, ellipses, parabolas, splines, etc. could be used as suited, especially for industrial applications. The reason we have restricted our discussion to straight lines is because this is the most generic element and all other types of features can be generated as compositions of straight line segments. This is actually anyway how all engineer have been brought up: divide a non-linear problem to small linear parts and solve them easily; then iterate to take care for the non-linear part. In any case, all the problems, degeneracies, and obtainable results discussed here are valid; only the analytics involved may be a little more complicated.

Although, as it has been shown, such an approach provides compatible accuracy with that obtained thus far by the classical point-based methodologies, it has several advantages and applications some of which may not be immediately apparent: Pragmatic possibility to fully automate the photogrammetric procedures, improved measurement accuracy in the context of full automation, universal application in fields ranging from mapping to motion estimation and robot vision. More apparent applications are such as better recognition of man-made objects, better modeling of non-frame sensors, automating map updating.

REFERENCES

Beyer, H., 1992. High-Precision Real-Time Photogrammetry. Ph.D. Dissertation, Institute of Geodesy and Photogrammetry, ETH-Zurich.

Beyer, H., T. Kersten, A. Streilein. 1992. Metric accuracy performance of solid-state camera systems, Proc. of SPIE OE/Technology'92 - Videometrics conference, Nov, 15-20, 1992, Boston, MA., SPIE Vol. 1820, pp. 103-110.

Buchanan, T., 1992a. On the critical set for photogrammetric reconstruction using line tokens in P3 (C). Geometriae Dedicata, 44, 223-232.

Buchanan, T., 1992b. Critical sets for 3D reconstruction using lines. In: G. Santini (ed.), Computer Vision - EECV '92, Springer Verlag, Berlin, pp. 730-738.

Burns, B.J., A.R., Hanson, E.M., Riseman, 1986. Extracting straight lines. IEEE Transc. on Pattern Analysis and Machine Intelligence, Vol. 8, No.4, pp. 425-455.

Bookstein, F.L., 1978. From biostereometrics to the comprehension of form, In: Applications of Human Biostereometrics, SPIE Proceedings, Vol. 166, pp. 74-79.

Canny, J., 1986. A computational approach to edge detection.IEEE Transc. on Pattern Analysis and Machine Intelligence, Vol. 8, No.6, pp. 679-698.

Dhome, M, Richetin, M., Lapreste, J.-T., Rives, G., 1989. Determination of the attitude of 3D objects from a single perspective view, IEEE Trans. Pattern Analysis and Machine Intelligence, 11(12), pp. 1265-1278.

Doehler, M., 1975. Verwendung von Pass-"Linien" anstelle von pass-"Punkten" in der Nhmildmessung. In: Festschrift K. Schwidefsky, Institut fur Fotogrammetrie und Topographie der Universitat Karlsruhe, pp. 39-45.

Faugeras, O., 1993. Three-Dimensional Computer Vision. A Geometrical Viewpoint. MIT Press, Cambridge, Mass.

Finsterwalder, R., 1991. Zur Verwendung von Passlinien bei photogrammetrischen Aufgaben. Zeitschrift f. Vermessungswesen, 116(2), pp. 60-66.

Finsterwalder, S. 1899. Die geometrischen Grundlagen der Photogrammetrie. Jahresbereicht der Deutchen Mathematiker - Vereinigung, VI(2), Teubner, Leipzig, Germany, pp. 1-41.

Finsterwalder, S., 1937. Die gemeinsame Ortung einer Mehzahl von Aufnahmen des gleichen Galaendes, Bildmessung u. Luftbiltwessen, 12(4), pp. 142-150.

Finstewalder, S., 1941. Die gemeinsame Koppelung dreier Luftaufnahmen desselben Gelaendes, Sitzungsbereichte der Bayerischen Akademie der Wissebschaften, Mathematischnaturwissen-schaftliche Abteilung, Sonderdruck, pp. 175-193.

Fryer, J.G., Goodin, D.J., 1989. In-flight aerial camera calibration from photography of linear features. Photogrammetric Engineering & Remote Sensing, 55(12), pp. 1751-1754.

Gruen, A., 1985. Adaptive Least Squares Correlation: A powerful image matching technique, South African Joutnal of Photogrammetry, Remote Sensing and Cartography, Vol. 14, No. 3, pp. 175-187.

Gruen, A., Beyer, H., 1990. DIPS II - Turning a standard computer workstation into a Digital Photogrammetric Station, International Archives of Photogrammetry and Remote Sensing, Vol. 28, Part 2, pp. 247-255.

Heikkinen, J., Laiho, A., 1992. The use of linear features as reference datum in digital map revision. In: International Archives of Photogrammetry & Remote Sensing, Washington DC, USA, vol. XXIX, Part B4, pp. 500-506.

Hekkila, J., 1991. Use of linear features in Digital Photogrammetry. The Photogrammetric Journal of Finland, 12(2), pp. 40-56.

Huang, T., 1990. Computer vision and Dynamic Scene Analysis. ISPRS Com. V Tutorial, ETH Zurich, Switzerland.

Horn, B., 1990. Relative Orientation, International Journal of Computer Vision, 4, pp. 59-78.

Karras, G.E., Patias, P., Petsa E., 1993. Experiences with rectification of non-metric digital images when ground control is not available. In: Proc. of CIPA XV International Symposium, Bucharest, Romania, September 22-26 (under publication).

Li, S.Z., Kittler, J., Petrou, M., 1992. Matching and recognition of road networks from aerial images, In: G. Santini (ed.), Computer Vision - ECCV '92, Lecture Notes in Computer Science, No. 588, Springer, Berlin, pp. 857-861.

Liu, Y., Huang, T.S., 1988. Estimation of rigid body motion using straight line correspondences. Computer Vision, Graphics and Image Processing, 43, pp. 37-52.

Liu, Y., Huang, T.S., 1990. Straight edge extraction and matching. In: Close-Photogrammetry meets Machine Vision, Gruen - Baltsavias (eds), SPIE Proc., vol 1395, pp. 612-619.

Liu, Y., Huang, T.S., Faugeras, O., 1990. Determination of camera location from 2-D to 3-D line and point correspondences. IEEE Trans. Pattern Analysis and Machine Intelligence, 12(1), pp. 28-37.

Luhmann, T., 1992. Bilderfassung in der Nahbereichsphotogrammetrie - Actuelle Tendenzen, Vermessungswesen und Raumordnung (VR 54/8), Dezember 1992, Wichmann-Verlag, Karlsruhe, pp. 400-410.

Masry, S.E., 1981. Digital mapping using entities: A new concept. Photogrammetric Engineering & Remote Sensing, 48(11), pp. 1561-1565.

Mikhail, E.M., 1993. Linear features for photogrammetric restitution and other object completion, In: Integrating Photogrammetric Techniques with Scene Analysis and Machine Vision, Proc. SPIE, Vol. 1944, pp. 16-30.

Mikhail, E.M., K., Weerawong, 1994, Feature-based photogrammetric object construction, Proc. of ASPRS/ACSM Annual Convention, Reno, Nevada, April 25-28, vol. 1, pp. 403-417.

McIntosh, J.H., Mutch, K.M., 1988. Matching straight lines. Computer Graphics Image Processing, Vol. 43, pp. 386-408.

Medioni, G., Nevatia, R., 1984. Matching images using linear features. IEEE Trans. Pattern Anal. Mach. Intell., Vol. PAMI-6, No. 6, Nov. 1984, pp. 675-685.

Mitiche, A., Habelrih, G., 1989. Interpretation of straight line correspondences using angular relations. Pattern Recognition, 22(3), pp. 299-308.

Mitichie, A., Faugeras, O., Aggarwal, J.K., 1989. Counting straight lines. Computer Vision, Graphics, and Image Processing, 47, pp. 353-360.

Mulawa, D., 1989. Estimation and Photogrammetric Treatment of Linear Features. PhD Dissertation, Purdue University, W. Lafayette, LA, USA.

Mulawa, D., Mikhail, E., 1988. Photogrammetric treatment of linear features, In: International Archives of Photogrammetry & Remote Sensing, Kyoto, Japan, vol. XXVII, Part B10, pp. 383-393.

Nalwa, V.S., T.O., Binford, 1986. On detecting lines. IEEE Transc. on Pattern Analysis and Machine Intelligence, Vol. 8, No.6, pp. 699-714.

Navab, N., 1993. Visual motion of lines and cooperation between motion and stereo, Ph.D. Thesis, University of Paris XI, Orsay.

Navab, N., Faugeras, O., Vieville, T., 1993. The critical sets of lines for camera displacement estimation: A mixed euclidean-projective and constructive approach. Proc. of the 4th International Conference on Computer Vision, Berlin, pp. 713-723.

Patias, P., 1993. Digital Imager and Sensor Information. In: Proc. of ISPRS Com. I Workshop on Digital Sensors and Systems, Trento, Italy, June 21-25, pp. 34-50.

Patias, P., D. Rossikopoulos, O. Georgoula. 1993. CIPA Test: "O. Wagner Pavillion". Preliminary Report. Presented at the CIPA XV International Symposium, Bucharest, Romania, September 22-26, (Executive Summary under publication in the proceedings).

Petsa E. (1994). Line Photogrammetry: Development and Testing of Line Photogrammetry Algorithms for Digital Photogrammetry applications. (PhD dissertation in progress).

Petsa E., Patias P., 1994(a). Formulation and assessment of straight line based algorithms for Digital Photogrammetry. In: Proc. of ISPRS Com. V Symposium, Melbourne, Australia, pp. 310-317.

Petsa E., Patias P., 1994(b). Relative orientation of image triples using straight line features. In: Proc. of ISPRS Com. III Symposium, Munich, Germany, pp. 663-669.

Petsa E., Patias P. 1994(c). Sensor attitude determination using linear features. In: Proc. of ISPRS Com. I Symposium, Como, Italy, pp. 62-70.

Price, K.E., 1984. Matching closed contours. In: Proc. 7th Intrn. Conference Pattern Recognition, pp. 990-992.

Schickler, W., 1992. Feature matching for outer orientation of single images using 3D wireframe control points. International Archives of Photogrammetry and Remote Sensing, Washington D.C, Vol. XXIX, Part 3, pp. 591-598.

Schwermann, W., 1994. Automatic image orientation and object reconstruction using straight lines in close-range Photogrammetry, In: Proc. of ISPRS Com. V Symposium, Melbourne, Australia, pp. 349-356.

Streilein, A. and S. Gaschen. 1994. Comparison of a S-VHS Camcorder and a High-Resolution CCD-Camera for use in Architectural Photogrammetry. Proc. of the ISPRS Intercongress Symposium, Melbourne, Australia, March 1-4, 1994, pp. 382-389.

Streilein, A., 1993. Application of a S-VHS Camcorder in Architectural Photogrammetry. Proc. of the CIPA XV International Symposium, Bucharest, Romania, September 22-26, (under publication).

Streilein, A., 1994. Towards automation in Architectural Photogrammetry: CAD-based 3D-feature extraction, ISPRS Journal of Photogrammetry and Remote Sensing, (under publication).

Strunz, G., 1992(a). Image orientation and quality assessment in feature based Photogrammetry. In: Robust Computer Vision, Forstner - Ruwiedel (eds), Wichman, Karlsruhe, pp. 27-40.

Strunz, G., 1992(b). Feature based image orientation and object reconstruction. In: International Archives of Photogrammetry & Remote Sensing, Washington DC, USA, vol. XXIX, Part B3, pp. 113-118.

Strunz, G., 1993. Bildorientierung und Objektrekostruktion mit Punkten, Linien und Flaechen. Deutsche Geodaetische Kommission, Reihe C, Nr. 408, Munchen, Germany.

Tommaselli, A.M.G., Tozzi, C.L., 1992. A filtering-based approach to eye-in-hand robot vision. In: International Archives of Photogrammetry & Remote Sensing, Washington DC, USA, vol. XXIX, Part 5, pp. 182-189.

Waldhausl, P., M. Brummer. 1989. Architectural Photogrammetry world-wide and by anybody with non-metric cameras?, Proc. of the CIPA XI International Symposium, October 1988, Sofia, Bulgaria. pp. 35-49.

Waldhausl, P. 1992. Defining the future of Architectural Photogrammetry, International Archives of Photogrammetry and Remote Sensing, Vol. 29, Bart B5, pp. 767-770

Waldhausl, P., C. Ogleby. 1994. 3x3 rules for simple photogrammetric documentation of architecture. Proc. of ISPRS Com. V Symposium, 1-4 March 1994, Melbourne, Australia, pp. 426-429.

Weng, J., Huang, T.S., Ahuja, N., 1992. Motion and structure form line correspondences: closed-form solution, uniqueness and optimization. IEEE Trans. Pattern Analysis and Machine Intelligence, 14(3), pp. 318-336.

Weng, J., Huang, T.S, Ahuja, N., 1993. Motion and structure from image sequences. Springer Series in Information Sciences, Vol. 29, Springer Verlag, Berlin.

Wenzhong, S., K. Temphli, 1994. Modelling positional uncertainly of line features in GIS. Proc. of ASPRS/ACSM Annual Convention, Reno, Nevada, April 25-28, vol. 1, pp. 606-705.

Wolfe, W.J., Mathis, D., Sklair, C.W., Margee, M., 1991. The perspective view of three points. IEEE Transc. Pattern Analysis and Machine Interlligence, 13(1), pp. 66-73.

Zhang, Z., Faugeras, O.D., 1991. Determining motion from 3D line segment matches: A comparative study. Image and Vision Computing, 9(1), pp. 10-19.

Zielinski, H., 1992. Line Photogrammetry with multuple images. In: International Archives of Photogrammetry & Remote Sensing, Washington DC, USA, vol. XXIX, Part B3, pp. 669-676.